THE JOURNAL OF PHYSICAL CHEMISTRY A

ARTICLE

pubs.acs.org/JPCA

Simulating the Formation of Sodium:Electron Tight-Contact Pairs: Watching the Solvation of Atoms in Liquids One Molecule at a Time

William J. Glover,[†] Ross E. Larsen,[‡] and Benjamin J. Schwartz*

Department of Chemistry and Biochemistry, University of California, Los Angeles, Los Angeles, California 90095-1569, United States

ABSTRACT: The motions of solvent molecules during a chemical transformation often dictate both the dynamics and the outcome of solution-phase reactions. However, a microscopic picture of solvation dynamics is often obscured by the concerted motions of numerous solvent molecules that make up a condensed-phase environment. In this study, we use mixed quantum/classical molecular dynamics simulations to furnish the molecular details of the solvation dynamics that leads to the formation of a sodium cation-solvated electron contact pair, (Na^+, e^-), in liquid tetrahydrofuran following electron photodetachment from sodide (Na^-). Our simulations reveal that the dominant solvent response is comprised of a series of discrete solvent molecular events that work sequentially to build up a shell of coordinating THF oxygen sites around the sodium cation end of the contact pair. With the solvent response described in terms of the sequential motion of single molecules, we are then able to compare the calculated transient absorption spectroscopy of the sodium species to experiment, providing a clear microscopic interpretation of ultrafast pump−probe experiments on this system. Our findings suggest that for solute−solvent interactions similar to the ones present in our study, the solvation dynamics is best understood as a series of kinetic events consisting of reactions between chemically distinct local structures in which key solvent molecules must be considered to be part of the identity of the reacting species.

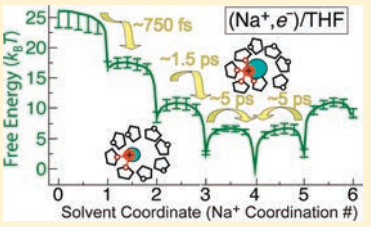

1. INTRODUCTION

Solvation dynamics, the response of a solvent to changes in a solute's electronic charge distribution, plays a central role in solution-phase chemical reactivity and is the dominant driving force underlying electron transfer and other chemical reactions.[1−3] Although there are ultrafast techniques for directly probing the motions of solvent molecules,[4−6] the most common experimental approaches to studying solvation dynamics involve measuring either the dynamic fluorescence Stokes shift[2,3,7] or photon echoes[8,9] from a molecular probe, usually an organic dye, dissolved in the liquid. With polyatomic solutes however, both solvation dynamics and internal relaxation of the probe can contribute to the experimental signals, and the fact that these processes often occur on similar time scales makes it challenging to interpret the results of such experiments.[10−12] Perhaps the simplest way to avoid this issue is to use an atomic solute as a probe of solvation dynamics: because atoms have only electronic degrees of freedom, any change in an atom's spectroscopic observables can result only from motions of the surrounding solvent molecules relative to the atom.

The chief difficulty with using atoms as probes of solvation dynamics is that of the few substances that dissolve atomically in common liquids, even fewer have an electronic structure that makes their spectroscopy readily accessible. We recently have found that it is possible to study the dynamics of sodium atoms in liquid tetrahydrofuran (THF) by creating the atoms in situ using photochemically driven charge transfer reactions.[13−16] We chose to study this system because in addition to being a convenient probe of solvation dynamics, the chemical nature of the sodium atom dissolved in liquid THF is interesting in its own right. Previous experiments have proposed[13,14,17−22] and simulations have confirmed[16,23] that at equilibrium, neutral sodium atoms in liquid THF are better thought of as (Na^+, e^-) tight-contact pairs (TCPs), species in which the valence electron is associated with the Na^+ cation but is also significantly displaced by the solvent, as seen in a representative molecular dynamics snapshot in Figure 1. Thus TCPs have equilibrium properties somewhere between those of solvated gas-phase-like atoms and cation-perturbed solvated electrons.

Ultrafast pump−probe experiments from both our laboratory[13] and others[21,24] have examined the formation of the sodium TCP in liquid THF by photodetaching an electron from sodide (Na^-). These experiments found that immediately following removal of sodide's excess electron, the neutral sodium atom that was left behind had an absorption spectrum peaked near 590 nm, the position of the gas-phase sodium D-line. This spectrum showed a small dynamic red-shift over the first ∼230 fs, and then underwent an isosbestic interconversion to form a new species, whose spectrum subsequently red-shifted on a ∼10-ps time scale to become the equilibrium sodium TCP spectrum in THF.[13] The initial spectrum of Na^0 was interpreted as resulting from a sodium atom that had a gas-phase-like absorption spectrum; this is because the newly created Na^0 only weakly interacts with the solvent, a result of the fact that the parent

Special Issue: A: Victoria Buch Memorial

Received: October 22, 2010
Revised: February 9, 2011
Published: March 23, 2011

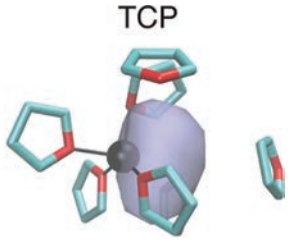

Figure 1. Molecular dynamics snapshot of the equilibrium neutral sodium tight-contact pair (TCP) in THF. The first solvation shell THF molecules are plotted as licorice, the Na^+ core as a black sphere (scaled to its ionic radius) and the valence electron is represented as a translucent blue isosurface enclosing 50% of the charge density. The black lines indicate THF oxygen sites within 3.65 Å of the Na^+. Reproduced with permission from ref 23. Copyright 2010 American Chemical Society.

sodide anion excludes a larger solvent cavity than is needed to accommodate the neutral. The initial rapid red shift was attributed to solvation of the Na^0, and the isosbestic point was assigned as indicative of a chemical reaction that converted the neutral atom into a nonequilibrium TCP. The nonequilibrium TCP was then observed to solvate, reaching equilibrium on a ~10-ps time scale.[13] These results raise a number of questions, including: given that the solute is an atom, what is the nature of the chemical reaction underlying the isosbestic point? Why is the time scale of the sodium TCP solvation nearly an order of magnitude slower than typical solvation time scales seen in liquid THF?[7,25] How does the presence of the electron in the sodium TCP alter the strong complexation of sodium cations by ether solvents and how is this reflected in its solvation dynamics?

Because of the chemical nature of the sodium TCP, it is not immediately clear whether the dynamical processes leading to its creation are controlled primarily by the solvation of either its sodium cation or its electron constituent, or whether the TCP should be considered a distinct species whose solvation cannot be described as the sum of its parts. Our group has previously explored the dynamics of solvated electrons in THF with ultrafast pump/probe spectroscopy; we found that solvation of excess electrons in liquid THF is essentially complete within ~450 fs following photoexcitation.[26−28] Mixed quantum/classical simulations on this system, also from our group, have suggested that this rapid solvation of excess electrons is controlled by the presence of naturally occurring voids within the THF solvent.[29] In contrast, the solvation of hard cations in complexing solvents like THF follows a completely different mechanism.[30] For example, MD simulations by Olender and Nitzan found that the solvation dynamics of Na^+ in various ether solvents is dominated by the formation of Na^+-oxygen dative bonds by the first-shell solvent molecules.[31] In ethyl−methyl ether in particular, the time scale associated with the motion of these nearby molecules to create the dative bonds was observed to be ~2 ps. Thus, the ~10-ps time scale seen in the solvation of Na^0/THF[13] is considerably longer than that of either of its components, suggesting complex dynamical solvent behavior that is due neither purely to the sodium cation nor the electron.

With the goal of better understanding the pump−probe experiments on Na^0/THF and answering the questions posed above, in this paper, we present the results of nonequilibrium molecular dynamics simulations of the formation of the sodium TCP in THF following electron photodetachment from Na^-. Our simulations build on our previous work exploring the equilibrium properties of this system[23] and are based on a mixed quantum/classical approach in which the valence electron of Na^0 is treated quantum mechanically and the Na^+ core and all the THF solvent molecules are treated classically. The quantum treatment of the valence electron is crucial to a realistic model of the sodium TCP, and also provides a means to calculate the transient absorption spectrum of the neutral sodium species during its solvation, affording a direct comparison with experimental pump−probe observables.

We find that our simulations reproduce the general features of the experimental transient absorption spectroscopy of Na^0/THF. In particular, we see that the spectrum of nascent Na^0 created after removing an electron from Na^- clearly results from gas-phase-like 3s → 3p transitions. Also in accord with experiment, our simulations of the subsequent spectral dynamics exhibit an isosbestic point, followed by a red shift on a ~10-ps time scale. We find that the features of the transient spectroscopy result from molecularly discrete changes in the solvation environment that are dominated by the solvation of the cation end of the TCP. In particular, the complex solvation dynamics of this system reflects the building up of a solvation shell of THF oxygens around the partially exposed Na^+ core, a process that occurs discretely, one solvent molecule at a time.[16] All of these observations have important implications for how to think about solvation dynamics, including the idea that solvation can be described as a series of simple first-order chemical reactions in which key solvent molecules are part of the identity of the reactants and products.

2. COMPUTATIONAL METHODS

To keep our simulation model as simple as possible, we make two basic assumptions about the photodetachment process of Na^- and the subsequent formation of the sodium TCP. First, we assume that upon photoexcitation, the valence electron ejected from Na^- is instantly detached and moves far enough away that it has no further influence on the dynamics of the neutral sodium species that remains behind. Second, we assume that the neutral sodium atom that remains is left in its electronic ground state and that it remains in this state for the duration of the nonequilibrium dynamics, that is, that the Born−Oppenheimer approximation holds. The first assumption is predicated on experiments that have shown that (for sufficiently high-energy excitation) not only is the sodide valence electron ejected several solvent shells away,[32] but also that the ejected electron and geminate neutral sodium atom lose correlation essentially instantly.[24] The second assumption is again supported by ultrafast pump−probe experiments, which found that immediately following photodetachment from Na^-, Na^0 had a transient absorption spectrum centered at the position of the gas-phase D-line.[13,21,24] Furthermore, our previous simulations of Na^-/THF showed that the excited-state electron density of sodide resembles that of ground-state Na^0 in the atomic core region (i.e., excitation of Na^- is essentially a one-electron transition).[33] Finally, the use of the Born−Oppenheimer approximation is justified by the presence of an energy gap of at least 0.6 eV between the ground and lowest excited states throughout the formation of the sodium TCP.[23]

With these assumptions, we executed 800 nonequilibrium Na^0 trajectories with initial classical positions and velocities extracted every 600 fs from a 240-ps long ground-state Na^-/THF trajectory (extended from the 80-ps long trajectory described in ref

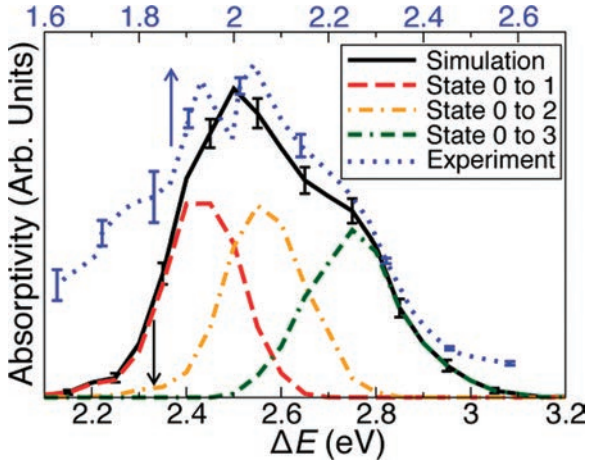

Figure 2. Simulated time-zero transient absorption spectrum of Na^0, following photodetachment of Na^-/THF, shown as the solid black curve. Errors bars represent the 95% confidence interval. Also shown are contributions to the calculated spectrum from transitions to the lowest three excited states (state 1: red dashed curve, state 2: orange dot-dashed, state 3: green dot-dash−dashed curve). The early time (0.38 ps) experimental Na^0 transient absorption spectrum, taken from ref 13, is plotted as the dotted blue curve (referenced to the upper axis) and scaled to the simulated absorption maximum. The excess absorption to the red of the peak in the experimental spectrum results from solvation dynamics during the 0.38-ps pump−probe delay; this relaxation has not yet taken place in the simulated time-zero spectrum.

33). Half of the nonequilibrium trajectories were generated by reversing the initial classical velocities. We instantly removed one of Na^-'s two valence electrons and propagated 32-ps long trajectories on the neutral sodium ground-state surface in the microcanonical ensemble with a 4-fs time step using the Verlet algorithm.[34] For consistency, our MQC simulation model was identical to that of our previous sodide study[33] with the obvious exception that the two quantum-mechanically treated valence electrons of sodide were replaced with a single Na^0 valence electron. The electronic ground-state wave function was expanded in a basis of $16 \times 16 \times 16$ grid points that spanned half the 32.50 Å simulation cell. To ensure that the wave function remained centered on the grid, particle positions were shifted every 200 fs in a manner described elsewhere.[35] To generate transient absorption spectra, solvent/solute configurations were saved every 12 fs during the nonequilibrium trajectories. These configurations then served as input to single-point calculations that solved for the lowest twenty adiabatic states in a basis of $32 \times 32 \times 32$ grid points spanning the entire simulation cell. The time-dependent absorption spectrum of the neutral sodium species was calculated in the inhomogeneous broadening limit according to:

$$I(E,t) \propto \sum_{i=1}^{19} |\mu_{0,i}(t)|^2 \Delta E_{0,i}(t) \delta(E - \Delta E_{0,i}(t)) \qquad (1)$$

where $\Delta E_{0,i}(t)$ and $\mu_{0,i}(t)$ are the energy gap and the transition dipole moments between the ground and ith excited state at time t after photodetachment, respectively. Equation 1 was evaluated with histogram bin widths of 0.05 eV. The spectra were then temporally convolved with a Gaussian function with a full width at half-maximum of 120 fs, corresponding to a typical time resolution of UV−vis pump−probe experiments.

3. RESULTS AND DISCUSSION

We begin our exploration of the nonequilibrium relaxation dynamics associated with the formation of the sodium TCP in liquid THF by first discussing the electronic properties of Na^0 immediately following its creation via electron photodetachment of Na^-. The time-zero spectrum of this species ($I(E,0)$ from eq 1) is plotted as the solid black curve in Figure 2; the various dashed and dot-dashed colored curves show the individual contributions to the total spectrum from the lowest three adiabatic excited states. The dotted blue curve plots the experimentally reconstructed absorption spectrum of Na^0 at the earliest available pump−probe time delay of 0.38 ps, taken from ref 13. To aid comparison, the experimental spectrum is plotted on a different energy scale (top axis) than the simulated spectrum (bottom axis) and the spectra have been scaled to have similar amplitudes.

The data in Figure 2 clearly support the experimental interpretation of this early time spectrum as arising from 3s → 3p transitions of a gas-phase-like sodium atom that only weakly interacts with its solvent environment.[13,24] This idea is also supported by the fact that the average wave function overlap of time-zero Na^0 's ground state (state 0) with that of a gas-phase sodium 3s state is almost unity ($|\langle\psi_0|\psi_{3s}^{Na^0_{gas}}\rangle| = 0.99$). In addition, the splitting of the 3p states (states 1−3) that we see in the simulation almost perfectly matches the splitting between the features seen in the experimental absorption spectrum at 1.93, 2.04, and 2.26 eV.[13,24] We note that despite this good agreement, our simulated spectrum has a substantial blue shift (of ∼0.5 eV) relative to experiment. This blue shift can be understood as resulting from excessive confinement of the excited-state 3p wave functions by the first solvent-shell THF molecules in the simulations; the average radius of gyration for these states is 2.9 Å compared to 3.4 Å for a gas-phase Na^0 in our model, suggesting that the initial solvent cavity radius is too small in our simulations. That the solvent cavity in our simulation might be too small is also consistent with our previous simulations using these same potentials that predicted a radius of gyration for Na^- that is smaller than the experimentally determined value.[33] Although this blue shift means that our simulated spectra are not in quantitative agreement with experiment, as we show below, our simulation model is more than adequate to understand the qualitative features of the experimental transient absorption spectroscopy of Na^0.

Figure 3 shows the time-resolved spectral dynamics of Na^0 during its solvation by liquid THF. Panel a shows simulated transient absorption spectra at times between 0.38 and 31.8 ps following removal of an electron from Na^-. For comparison, the experimentally reconstructed Na^0 absorption spectra over a similar time range are shown in panel c; we note that the energy scales in panels a and c are different because the experiments were unable to probe the transient spectrum to the red of 1.63 eV.[13] Although there is not quantitative agreement between the simulated and experimental spectra (largely because of the blue shift of the simulated time-zero spectrum, discussed above), the qualitative features of the spectral dynamics are well-captured by our simulations. Importantly, our simulations reproduce the slow spectral red shift that is seen experimentally, with solvation dynamics continuing for nearly 30 ps following photodetachment. In addition to reproducing the slow red shift of the experimental spectrum, our simulations also capture the isosbestic behavior seen experimentally (panel d): panel b enlarges

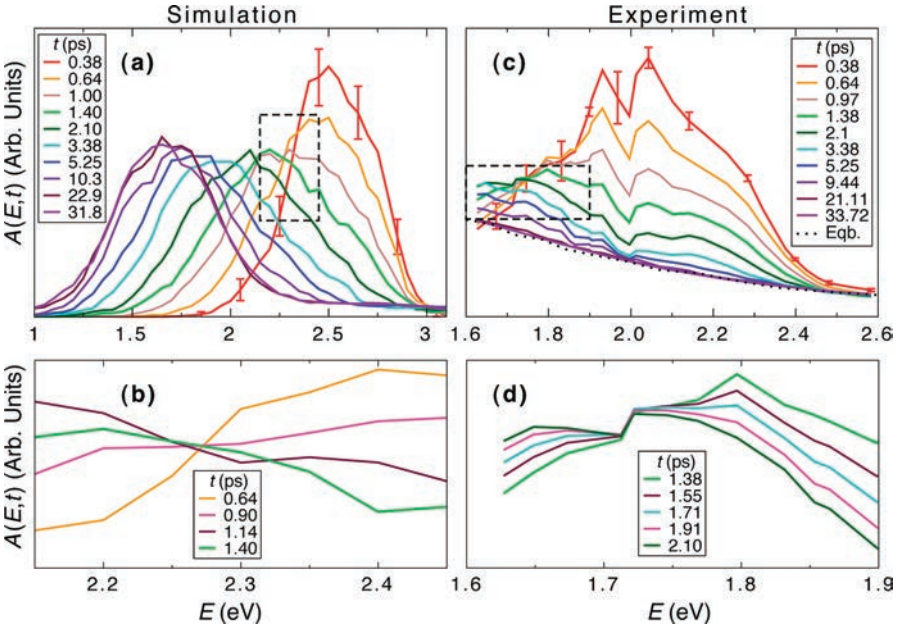

Figure 3. Transient absorption spectra, $I(E,t)$, of Na^0 following photodetachment of Na^-/THF. Panel a shows the simulated spectra at representative times from 0.38 to 31.8 ps, following electron detachment, calculated via eq 1 with a 0.05-eV bin width and convoluted temporally with a Gaussian function with a full width at half-maximum (fwhm) of 120 fs. Error bars representing the 95% confidence interval are shown for the earliest-time spectrum (red curve); the statistical uncertainty is similar in magnitude across the time series. Panel b zooms into the region indicated by dashed lines in panel a, showing the dynamics between 0.64 and 1.40 ps on an expanded scale, where evidence for an isosbestic point can be seen around 2.27 eV. Panel c shows the experimentally reconstructed transient absorption spectra of Na^0 at representative times following photodetachment of Na^-/THF, taken from ref 13. The black dotted curve shows the steady-state absorption of an equilibrium (Na^+, e^-) tight-contact pair.[19] The experimental spectra were recorded only between 1.63 and 2.58 eV, so the energy scale of panel c is different to that of the simulated spectra shown in panel a. Panel d expands the region indicated by dashed curves in panel c, where the experimental isosbestic point is seen.

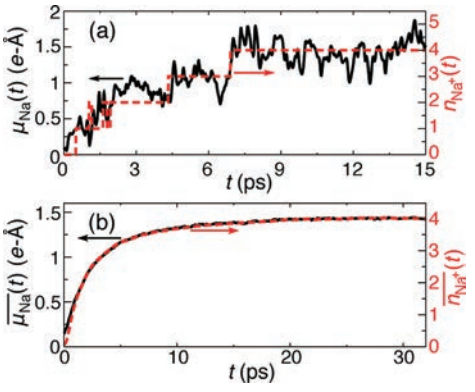

Figure 4. Correlation of the instantaneous dipole moment of the neutral atomic sodium species in liquid THF with the solvent coordination number of the sodium cation core, n_{Na^+}. Panel a shows a time trace of the instantaneous dipole moment magnitude, $\mu_{Na}(t)$, of the sodium atom (solid black curve, left axis) from a representative nonequilibrium trajectory. Plotted on a different scale (right axis) as the dashed red curve is n_{Na^+}; the sudden changes in $\mu_{Na}(t)$ are correlated with changes in n_{Na^+}, reflecting the discrete nature of solvation in this system. Panel (b) plots nonequilibrium-ensemble-averaged values of $\overline{\mu_{Na}}(t)$ (black curve, left axis) and $\overline{n_{Na^+}}(t)$ (dashed red curve, right axis).

the intermediate-time region of the calculated spectroscopy, showing clear isosbestic behavior within the statistical uncertainty of the simulations. The experimental assignment of this isosbestic behavior was that it reflected the simple chemical interconversion of two species.[13] What we show next, however, is that the origin of this isosbestic behavior reflects some considerably more complex underlying chemical processes.

We believe that the best way to understand the origin of the slow solvation and isosbestic point seen in the spectral dynamics is as a result of specific changes in the chemical nature of the sodium TCP that occur through solvation of the cation end of the TCP.[23] In previous simulation work examining the equilibrium properties of this species, we found that the reason the TCP valence electron is displaced is because four (on average) THF oxygen sites form a tight coordination shell around the Na^+ end of the TCP.[23] We also found that cation coordination numbers three and five are readily thermally accessible at room temperature, and that integer coordination numbers one through six correspond to free energy local minima that are separated by barriers of a few k_BT. This suggests that neutral sodium species with different cation coordination numbers are chemically distinct,[23] an interpretation reinforced by our recent experimental observation that these species with differing coordination numbers have measurably different absorption spectra.[16] The implication of this is that the solvation dynamics of the sodium TCP, as reflected in the spectral dynamics seen in Figure 3, is best described as a series of chemical interconversions between neutral sodium species with different solvent coordination numbers rather than resulting from concerted solvent relaxation.

That the solvation dynamics of Na^0 is controlled by sequential changes in the solvent coordination number of Na^+ is apparent directly from the simulation trajectories. Figure 4a plots the time trace of the sodium atom's dipole moment magnitude, μ_{Na} (solid black curve), for a single representative trajectory. At $t = 0$, $\mu_{Na} \approx 0$ because of the approximately spherical solvation environment

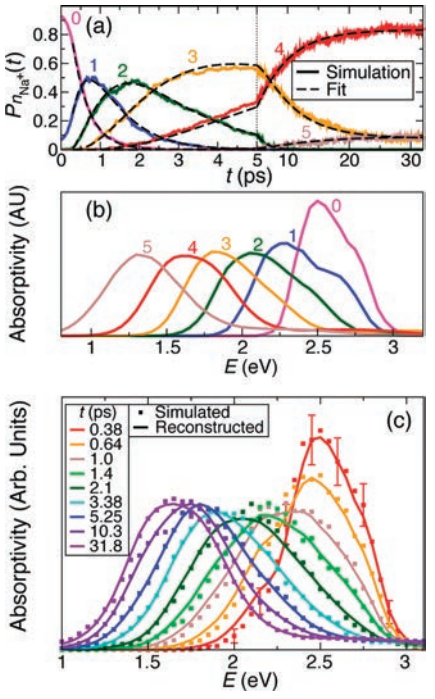

Figure 5. Solvation dynamics of Na^0 understood through changes in the Na^+ coordination number, n_{Na^+}. Panel a shows the population dynamics of n_{Na^+} (indicated by the number above each solid curve). For clarity, the time axis scale is split into an early time region (0−5 ps) and long-time region (5−32 ps). The black dashed curves show a least-squares fit of the reaction scheme given in eq 2 to the population dynamics; see Appendix for details. Panel b shows the simulated electronic absorption spectra for each n_{Na^+} (indicated by the number above each spectrum) as a nonequilibrium ensemble average during the solvation of Na^0 . Panel c compares the transient spectroscopy computed by multiplying the spectra in panel b by the relative population of each species at each time given in panel a (various colored solid curves), to the total simulated transient spectroscopy (various colored squares; same data as in Figure 3a).

of Na^-. As solvation progresses, the valence electron of sodium is increasingly displaced from the Na^+ core until μ_{Na} fluctuates around the new equilibrium value of ∼1.4 e-Å, corresponding to the equilibrium (Na^+, e^-) species. However, the changes in μ_{Na} do not occur smoothly; rather, there are clear discrete events that involve sudden changes in μ_{Na}. As the dashed red curve in Figure 4a shows, these events are correlated with sequential changes in the coordination number of the Na^+, n_{Na+} (defined[23] as the number of strongly coordinating THF oxygen sites that are within 3.65 Å of the Na^+).

Further evidence that changes in the coordination number of Na^+ represent the dominant solvation mechanism is seen in the temporal behavior of the nonequilibrium-ensemble-averaged quantities, $\overline{\mu_{Na}}(t)$ and $\overline{n_{Na^+}}(t)$, plotted as the black and dashed red curves respectively in Figure 4b. This figure shows that the slow ∼10-ps solvation time scale observed in the transient absorption spectroscopy of Na^0/THF is clearly reflected in the evolution of $\overline{n_{Na^+}}(t)$, which remarkably is directly proportional to $\overline{\mu_{Na}}(t)$ for the entire solvation process beyond $t \approx 1$ ps. Thus, given that the dipole moment of the atomic sodium species is a direct measure of the electron displacement that defines the extent of reaction between Na^0 and (Na^+, e^-), Figure 4 shows clearly that this process is driven essentially exclusively by discrete changes in the local Na^+ coordination by the solvent.

To explore the coordination number changes underlying the solvation dynamics of Na^0/THF in more detail, in Figure 5a, we plot the population dynamics of each Na^+ coordination number present during the nonequilibrium solvation as the various solid colored curves. In this figure, the population $P_{n_{Na^+}}(t)$ represents the fraction of the 800 nonequilibrium trajectories in which the Na^+ has coordination number n_{Na^+} at time t. At $t = 0$, we see that Na^+ is predominantly uncoordinated; however, a small population of $n_{Na^+} = 1$ is also seen. This initial coordination results from the fact that the Na^+ core of the parent Na^- ion is solvated occasionally by the oxygen end of one THF molecule, in a manner similar to that seen in our previous simulations of Na^- in aqueous solution.[35] As time progresses, the population of $n_{Na^+} = 1$ increases because a single THF molecule brings its oxygen site into coordination with the Na^+, leading to a corresponding decrease in the $n_{Na^+} = 0$ population. The $n_{Na^+} = 2$ population then rises as the oxygen site on a second solvent molecule coordinates, leading to a decay in the $n_{Na^+} = 1$ population, and so forth. This continues until the $n_{Na^+} = 4$ population reaches a dynamic equilibrium with $n_{Na^+} = 3$ and $n_{Na^+} = 5$ at $t \approx 30$ ps. The dashed black curves in Figure 5a are a global fit of a simple model, which is described in more detail in the Appendix, that represents the changing populations by a set of consecutive first-order kinetic reactions:

$$\mathbf{0} \xrightarrow{0.42\text{ps}} \mathbf{1} \xrightarrow{0.74\text{ps}} \mathbf{2} \xrightarrow{1.5\text{ps}} \mathbf{3} \underset{61\text{ps}}{\overset{5.8\text{ps}}{\rightleftharpoons}} \mathbf{4} \underset{5.1\text{ps}}{\overset{48\text{ps}}{\rightleftharpoons}} \mathbf{5} \qquad (2)$$

where the boldface integers are shorthand for the different coordination numbers, and the time scales are the inverse rate constants for each first-order step. The fact that such a simple kinetic model fits the calculated population dynamics so well provides strong support for the idea that the solvation dynamics of this system is best thought of as a series of chemical interconversions between independent species with different solvent coordination numbers.

To make a concrete connection between the coordination number population dynamics of Figure 5a and the spectral dynamics seen in Figure 3, we plot the absorption spectrum of each of the different solvent-coordinated neutral sodium species in Figure 5b; these were determined as a time-average of the spectrum associated with each coordination number occupied during the nonequilibrium trajectories. This figure shows that the spectrum of the neutral sodium species red shifts by ∼0.25 eV with each increase in coordination number. These nonequilibrium spectra are almost identical to those seen at equilibrium (cf., Figure 7 of ref 23), with the small differences likely being a result of the slightly different definitions of coordination number in these two studies. As at equilibrium, we can explain the red shift with increasing coordination as a progressive destabilization of sodium's 3s state relative to the 3p states because of increased displacement of the electron from the sodium cation core.[23] The connection between coordination number population kinetics and spectroscopy is made clear if we simply multiply the spectrum of each coordination species, $I_i(E)$, by its population dynamics, $P_i(t)$

$$I_r(E,t) = \sum_{i=0}^{5} I_i(E) \times P_i(t) \qquad (3)$$

As shown in Figure 3c, the time-dependent spectroscopy calculated this way (solid curves) agrees within error to the full calculated spectroscopy (squares). Clearly, if we think of sodium

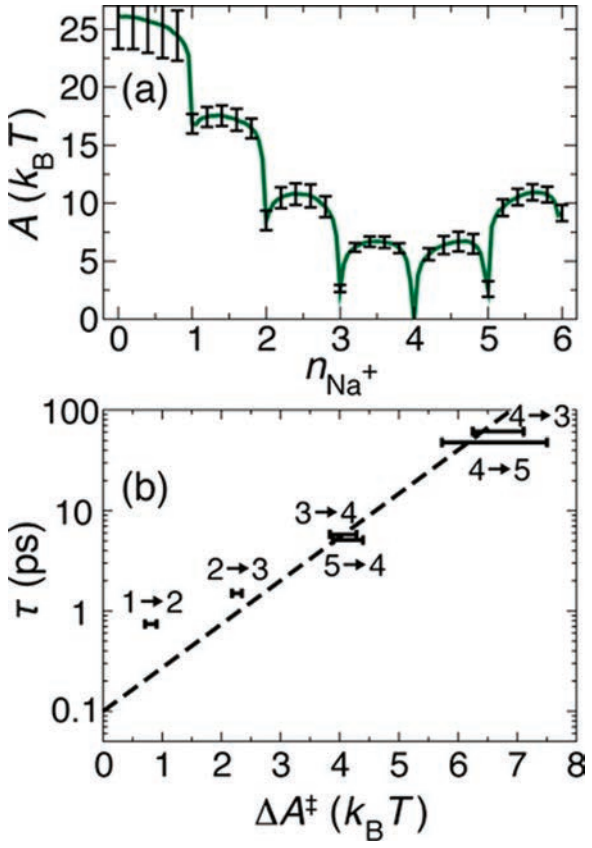

Figure 6. Solvation dynamics of Na^0 can be related to the potential of mean force along the solvent coordination number. Panel a shows the free energy, A, of a neutral sodium atom in liquid THF as a function of a continuously defined Na^+ coordination number, n_{Na^+}, reproduced from ref 23. Panel b plots the six different coordination number interconversion time scales, τ, extracted from the model used to fit the data in Figure 5a (see Appendix for details), against the free energy barrier height, $\Delta A^{\ddagger}$, extracted from panel a. The coordination number interconversions are indicated by the numbers over each data point and the $0 \rightarrow 1$ transition is omitted as this interconversion is barrier-less. Error bars in the free energy barriers correspond to 95% confidence intervals estimated from sampling the barrier heights in five blocks of the data from ref 23. The dashed line shows a fit-by-eye to $\tau/\text{ps} = 0.1 \exp(\Delta A^{\ddagger}/k_B T)$ (note the semilog scale). The roughly exponential relationship between the interconversion time scales and barrier heights follows from transition state theory, as described in the text.

TCPs with distinct solvent coordination numbers as chemically independent species with distinct spectra, then the entire solvent relaxation process can be described as a series of simple, first-order chemical interconversion reactions, as given by eq 2.

The fact that the full spectral dynamics of this system can be explained simply by changes in the solvent coordination number of the cation provides a molecular-level interpretation of the experimentally observed solvent relaxation. The initial spectrum of Na^0 is mainly that of the zero-coordinated species, which in our simulations absorbs at ~2.5 eV. This species rapidly converts into the singly coordinated species, which has a broader absorption peaked at ~2.25 eV, giving rise to the rapid initial red shift seen experimentally on the ~0.23-ps time scale.[13,36] Next, the isosbestic point, seen both in our simulations and in experiment, is consistent with the slower subsequent interconversion between the spectroscopically distinct singly- and doubly coordinated species.[37] The remaining long-time solvation red shift can be assigned to the increasingly slower sequential interconversions between coordination numbers 2−5; these interconversions do not result in isosbestic points because the time scales on which they take place strongly overlap.

Finally, we can understand the nonequilibrium solvation dynamics of Na^0/THF in light of the way its free energy changes with solvent coordination number, which we calculated in our previous equilibrium study of this system[23] and which is reproduced in Figure 6a. In particular, the free energy, A, exhibits local minima at integer values of the coordination number, with the lowest minimum at $n_{Na^+} = 4$, corresponding to the dominant equilibrium sodium TCP species. The presence of barriers of a few $k_B T$ between the integer coordination numbers is the reason they should be thought of as chemically distinct species and also indicates that the interconversion between these species is an activated process. Indeed, as Figure 6b shows, the inverse rates, τ, for coordination number interconversion (extracted from Figure 5a) are roughly consistent with values predicted from transition state theory, $\tau = \tau_0 \exp(\Delta A^{\ddagger}/k_B T)$, where $\Delta A^{\ddagger}$ is the free energy barrier height for the interconversion, extracted from Figure 6a, and a best-fit line gives an inverse attempt frequency of $\tau_0 = 0.1$ ps.[38] Thus, the progressively slower interconversions between coordination numbers (from low to high) are a direct result of increasingly higher free energy barriers with increasing coordination number, such that the slowest components of the solvation dynamics occur on time scales of tens of picoseconds.

4. CONCLUSIONS

In the Introduction of this paper, we posed three questions concerning the experimental observations of the solvation of (Na^+, e^-) TCPs in liquid THF: (1) Given that the solute is an atom, what is the nature of the chemical reaction underlying the observed isosbestic point?[13] (2) Why is the time scale of the sodium TCP solvation nearly an order of magnitude slower than typical solvation time scales seen in liquid THF?[7,25] (3) How does the presence of the electron in the sodium TCP alter the strong complexation of sodium cations by ether solvents and how is this reflected in its solvation dynamics? The results presented above leave us in a position to directly address these questions. For the first question, we see that the complex solvation dynamics associated with the formation of the TCP results from the fact that the first solvation shell THF molecules determine the chemical identity of the TCP species. The equilibrium TCP's formation from an atomic-like Na^0 is dominated by interconversions between chemically distinct sodium species differing in the number of THF oxygens coordinated to the cation end of the TCP. These interconversions manifest experimentally as an isosbestic point in the transient spectroscopy as well as the distinct structures observed in transient hole-burning experiments on this same system.[16] For the second question, we now understand that the slow relaxation time scale for reaching equilibrium arises from the presence of substantial free energy barriers (up to ~7 $k_B T$) associated with interconversions between the sodium species with differing coordination numbers. Interestingly, the nearly symmetrical free energy curve going from coordination number 4 (the thermodynamically most stable) to 3 and 4 to 5 suggests that at equilibrium, solvent exchange proceeds via both associative and dissociative mechanisms.[30] Finally, we can answer the third question by

noting that although our simulations reveal that the solvation dynamics of the TCP is dominated by the complexation of the Na^+ core, the electron is clearly more than just a spectator in the reaction, as evidenced by the slower solvation time scales of the TCP relative to bare sodium cations in ether solvents.[31] As we showed previously,[23] the degree of cation coordination in the TCP is controlled by a balance between the cost of (partially) ionizing the electron from the cation core and the solvation energy gained from forming strong Na^+-oxygen dative bonds. Clearly, the solvation dynamics as well as the energetics of the TCP also reflects this balance.

Although we chose to study the dynamics of the neutral sodium TCP in THF to make close contact with experiment, it is worth noting that the strengths and duration of the solvent−solute interactions that characterize the TCP in THF are similar to those that define systems of broader interest, for example, solute−solvent hydrogen-bond interactions in aqueous environments[39] and the hydrogen-bonding and electrostatic interactions between residues in proteins .[40−42] Thus, for many systems where specific local interactions dominate or are at least as important as long-range interactions, we expect that restructuring via a relatively small number of local interactions will dominate solvation in a similar fashion as it does for the sodium TCP. It would be interesting to explore in future work the extent to which our findings can be generalized to other systems of interest.

APPENDIX: FITTING A SEQUENTIAL KINETICS MODEL OF THE NA^+ COORDINATION NUMBER POPULATION DYNAMICS

In this appendix, we provide details of how we modeled the population dynamics of the Na^+ coordination numbers (solid curves in Figure 5a) as a set of sequential interconversions (eq 2). Our starting point was noticing that only coordination numbers 3, 4, and 5 have appreciable populations in the tight-contact pair (TCP) at equilibrium; furthermore, coordination number 6 was not populated in any of the non-equilibrium simulations (consistent with it being ~9 k_BT higher in free energy compared to coordination number 4). Thus, we assumed that all interconversions were irreversible, except for the interconversions between coordination numbers 3 and 4, and 4 and 5, leading to the following set of coupled first-order kinetic equations (written in matrix form):

$$\begin{pmatrix} \dot{P}_0 \\ \dot{P}_1 \\ \dot{P}_2 \\ \dot{P}_3 \\ \dot{P}_4 \\ \dot{P}_5 \end{pmatrix} = \begin{pmatrix} -\tau_{0\to1}^{-1} & 0 & 0 & 0 & 0 & 0 \\ \tau_{0\to1}^{-1} & -\tau_{1\to2}^{-1} & 0 & 0 & 0 & 0 \\ 0 & \tau_{1\to2}^{-1} & -\tau_{2\to3}^{-1} & 0 & 0 & 0 \\ 0 & 0 & \tau_{2\to3}^{-1} & -\tau_{3\to4}^{-1} & \tau_{4\to3}^{-1} & 0 \\ 0 & 0 & 0 & \tau_{3\to4}^{-1} & -\tau_{4\to3}^{-1} - \tau_{4\to5}^{-1} & \tau_{5\to4}^{-1} \\ 0 & 0 & 0 & 0 & \tau_{4\to5}^{-1} & -\tau_{5\to4}^{-1} \end{pmatrix} \begin{pmatrix} P_0 \\ P_1 \\ P_2 \\ P_3 \\ P_4 \\ P_5 \end{pmatrix} \quad (4)$$

where $\dot{P}_i$ is the rate of change of coordination number i's population and $\tau_{i\to j}$ is the inverse rate constant for the interconversion of coordination number i to j. Equation 4 was solved by numerical diagonalization,[43] and the resulting solution was fit to the simulated population dynamics by optimizing the seven rate constants with the method of least squares.[44] To avoid a poor fit to the early-time inertial region of the population dynamics, we fit only the simulation results from 300 fs onwards and we constrained the populations at this time to match the simulation values: $P_0(300\text{ fs}) = 0.74$, $P_1(300\text{ fs}) = 0.25$, $P_2(300\text{ fs}) = 0.01$, and $P_{i>2}(300\text{ fs}) = 0$. The resulting optimized inverse rate constants are shown in eq 2 and the fit is shown as the dashed curves in Figure 5a.

AUTHOR INFORMATION

Corresponding Author

*E-mail: schwartz@chem.ucla.edu.

Present Addresses

[†]Department of Chemistry, Stanford University, Stanford, CA 94305-5080

[‡]Center for Scientific Computing, National Renewable Energy Laboratory, Golden, CO 80401-3305

ACKNOWLEDGMENT

This work was supported by the National Science Foundation under Grant No. CHE-0908548 and the American Chemical Society Petroleum Research Fund under Grant No. 45988-AC,6. We also gratefully acknowledge the UCLA Institute for Digital Research and Education for allocating computer time for the calculations presented in this paper and we thank Arthur Bragg for insightful discussions.

REFERENCES

(1) Marcus, R. A. *Rev. Mod. Phys.* **1993**, *65*, 599–610.
(2) Maroncelli, M. *J. Mol. Liq.* **1993**, *57*, 1–37.
(3) Stratt, R. M.; Maroncelli, M. *J. Phys. Chem.* **1995**, *100*, 12981–12996.
(4) Castner, E. W.; Maroncelli, M. *J. Mol. Liq.* **1998**, *77*, 1–36.
(5) Loughnane, B. J.; Scodinu, A.; Farrer, R. A.; Fourkas, J. T.; Mohanty, U. *J. Chem. Phys.* **1999**, *111*, 2686–2694.
(6) Underwood, D. F.; Blank, D. A. *J. Phys. Chem. A* **2003**, *107*, 956–961.
(7) Horng, M. L.; Gardecki, J. A.; Papazyan, A.; Maroncelli, M. *J. Phys. Chem.* **1995**, *99*, 17311–17337.
(8) Fleming, G. R.; Cho, M. *Annu. Rev. Phys. Chem.* **1996**, *47*, 109–134.
(9) de Boeij, W.; Pshenichnikov, M.; Wiersma, D. *Annu. Rev. Phys. Chem.* **1998**, *49*, 99–123.
(10) Fee, R. S.; Maroncelli, M. *Chem. Phys.* **1994**, *183*, 235–247.
(11) Schwartz, B. J.; Rossky, P. J. *J. Phys. Chem.* **1995**, *99*, 2953.
(12) Larsen, D. S.; Ohta, K.; Xu, Q. H.; Cyrier, M.; Fleming, G. R. *J. Chem. Phys.* **2001**, *114*, 8008–8019.
(13) Cavanagh, M. C.; Larsen, R. E.; Schwartz, B. J. *J. Phys. Chem. A* **2007**, *111*, 5144–5157.
(14) Bragg, A. E.; Schwartz, B. J. *J. Phys. Chem. A* **2008**, *112*, 3530–3543.
(15) Bragg, A. E.; Cavanagh, M. C.; Schwartz, B. J. *Science* **2008**, *321*, 1817–1822.
(16) Bragg, A. E.; Glover, W. J.; Schwartz, B. J. *Phys. Rev. Lett.* **2010**, *104*, 233005.
(17) Bockrath, B.; Dorfman, L. M. *J. Phys. Chem.* **1973**, *77*, 1002.
(18) Fletcher, J. W.; Seddon, W. A. *J. Phys. Chem.* **1975**, *79*, 3055–3064.
(19) Seddon, W. A.; Fletcher, J. W.; Sopchyshyn, F. C.; Selkirk, E. B. *Can. J. Chem.* **1979**, *57*, 1792–1800.
(20) Piotrowiak, P.; Miller, J. R. *J. Am. Chem. Soc.* **1991**, *113*, 5086–5087.
(21) Shoshana, O.; Lustres, J. L. P.; Ernsting, N. P.; Ruhman, S. *Phys. Chem. Chem. Phys.* **2006**, *8*, 2599–2609.

(22) Cavanagh, M. C.; Young, R. M.; Schwartz, B. J. *J. Chem. Phys.* **2008**, *129*, 134503.
(23) Glover, W. J.; Larsen, R.; Schwartz, B. J. *J. Phys. Chem. B* **2010**, *114*, 11535–11543.
(24) Shoshanim, O.; Ruhman, S. *J. Chem. Phys.* **2008**, *129*, 044502.
(25) Bedard-Hearn, M. J.; Larsen, R. E.; Schwartz, B. J. *J. Phys. Chem. B* **2003**, *107*, 14464–14475.
(26) Martini, I. B.; Barthel, E. R.; Schwartz, B. J. *J. Chem. Phys.* **2000**, *113*, 11245–11257.
(27) Martini, I. B.; Schwartz, B. J. *Chem. Phys. Lett.* **2001**, *360*, 22–30.
(28) Bragg, A. E.; Schwartz, B. J. *J. Phys. Chem. B* **2008**, *112*, 483–494.
(29) Bedard-Hearn, M. J.; Larsen, R. E.; Schwartz, B. J. *J. Chem. Phys.* **2006**, *125*, 194509.
(30) Helm, L.; Merbach, A. E. *Chem. Rev.* **2005**, *105*, 1923–1960 and references therein.
(31) Olender, R.; Nitzan, A. *J. Chem. Phys.* **1995**, *102*, 7180–7196.
(32) Barthel, E. R.; Martini, I. B.; Keszei, E.; Schwartz, B. J. *J. Chem. Phys.* **2003**, *118*, 5916–31.
(33) Glover, W. J.; Larsen, R. E.; Schwartz, B. J. *J. Chem. Phys.* **2010**, *132*, 144102.
(34) Allen, M. P.; Tildesley, D. J. *Computer Simulation of Liquids*; Oxford University Press: London, U.K., 1992.
(35) Glover, W. J.; Larsen, R. E.; Schwartz, B. J. *J. Chem. Phys.* **2008**, *129*, 164505.
(36) The transient absorption spectrum of Na^0 does not show an isosbestic point corresponding to the interconversion of zero to singly coordinated Na^+, which could reflect the lack of a barrier separating the zero- and one-coordinated species, resulting in a continuous shift in the spectral dynamics. In addition, there are likely other aspects to the early-time solvation dynamics, such as changes in the size of the solvent cavity and solvent reorientations (see ref 25) that could obscure the zero-to-one interconversion isosbestic point.
(37) It is possible that the isosbestic point seen in Figure 3 is not strictly isosbestic. As Figure 5c shows, during the apparent isosbestic point in the simulated spectrum at $t \approx 1$ ps, more than two species are interconverting (coordination numbers 0, 1, and 2 all have appreciable population). Nevertheless, the presence of even a quasi-isosbestic point provides support to our interpretation that the solvation dynamics of Na^0 is dictated by discrete changes in the number of coordinating THF molecules.
(38) The deviations from the fit in Figure 6b seen for interconversions $1 \rightarrow 2$ and $2 \rightarrow 3$ are most likely a consequence of barrier recrossings for these interconversions, evidence of which is seen in Figure 4a.
(39) Kropman, M. F.; Bakker, H. J. *Science* **2001**, *291*, 2118–2120.
(40) Lim, M.; Hamm, P.; Hochstrasser, R. M. *Proc. Natl. Acad. Sci.* **1998**, *95*, 15315.
(41) Mukherjee, P.; Kass, I.; Arkin, I. J.; Zanni, M. T. *Proc. Natl. Acad. Sci.* **2006**, *103*, 3528.
(42) Gamin, Z.; Chung, H. S.; Smith, A. W.; DeFlores, L. P.; Jones, K. C.; Tokmakoff, A. *Acc. Chem. Res.* **2008**, *41*, 432.
(43) Anderson, E.; Bai, Z.; Bischof, C.; Blackford, S.; Demmel, J.; Dongarra, J.; Du Croz, J.; Greenbaum, A.; Hammarling, S.; McKenney, A.; Sorensen, D. *LAPACK Users' Guide*, 3rd ed.; Society for Industrial and Applied Mathematics: Philadelphia, PA, 1999.
(44) Marquardt, D. W. *SIAM J. Appl. Math.* **1963**, *11*, 431–441.